ELSEVIER

Contents lists available at ScienceDirect

Computational Materials Science

journal homepage: www.elsevier.com/locate/commatsci





Strain tuned thermal conductivity reduction in Indium Arsenide (InAs) – A first-principles study

Rajmohan Muthaiah*, Jivtesh Garg

School of Aerospace and Mechanical Engineering, University of Oklahoma, Norman, OK 73019, USA

ARTICLE INFO

Keywords: Indium arsenide Semiconductor Biaxial strain Thermoelectric materials Phonon-phonon scattering

ABSTRACT

Indium based semiconductors are promising materials for thermoelectric devices. Efficiency of a thermoelectric material can be improved by minimizing the lattice thermal conductivity (k). Using first-principles calculations, we report ~20% reduction in in-plane thermal conductivity of Indium arsenide (InAs) with 3% biaxial compressive strain. At 300 K, the bulk thermal conductivity of 33.85 Wm $^{-1}$ K $^{-1}$ computed for unstrained indium arsenide (InAs) is reduced to 27 Wm $^{-1}$ K $^{-1}$ for the 3% biaxially strained InAs. Systematic analysis of the effect of applied biaxial strain on phonon group velocities and phonon scattering rates of longitudinal (LA) and transverse (TA) acoustic phonon modes is carried out. Our results shed a light on modulating thermal conductivity of materials through biaxial strain.

1. Introduction

Thermoelectric (TE) materials, which are capable of converting heat into electric current through Seebeck effect, draw significant attention among researchers due to the eco-friendly energy conversion [1–3]. The efficiency of a thermoelectric material is expressed by dimensionless figure of merit (ZT = $\sigma S^2 T/k$), where σ is the electrical conductivity, S is the Seebeck coefficient, T is the temperature and k is the thermal conductivity [5]. High ZT can be obtained by either increasing the power factor (σS^2) [6,7] or by minimizing lattice thermal conductivity [8,9]. Over the years, several materials have been reported with high thermoelectric performance such as PbTe [10], SnSe [11], Bi₂Te₃ [12], PbS and SiGe alloys [13]. PbTe and PbS are used as thermoelectric materials because of their very good electrical conductivity and low thermal conductivity [14,15]. The key strategy to improve figure of merit without affecting electrical conductivity and Seebeck coefficient is to reduce the lattice thermal conductivity. Thermal conductivity can be reduced by introducing disorder which leads to increase in phonon scattering. Strain engineering is another promising approach to modify thermal conductivity by controlling the phonon bandgap between acoustic and optical phonons. In a recent work, increase in thermal conductivity of BP is reported through biaxial compressive strain [16]. Increase and decrease in thermal conductivity of wurtzite gallium nitride have been reported for 5% biaxial compression and biaxial tension respectively [17]. Effects of biaxial strain on thermal conductivity

modulation is yet to be explored for thermoelectric materials.

Indium Arsenide (InAs) is a direct band gap semiconductor with high electron mobility and is used for field effect transistors, quantum-well structures, and substrate for magnetic field sensors, lasers and detectors because of its large Hall coefficient [18,19]. Indium Arsenide based thermoelectric materials [20,21] with a power factor of 10^{-3} W/mK [2] were observed over a temperature range of 300 to 600 K. An order of increase in power factor was observed at 20 K in InAs nanowires [22]. In this work, we report 20% reduction in in-plane thermal conductivity of InAs through 3% biaxial compressive strain. Reduction in thermal conductivity is due to increase in phonon scattering rate and decrease in phonon group velocities of both TA and LA phonons.

2. Methodology

Lattice thermal conductivity(k) of Indium Arsenide (InAs) is calculated using first principles calculations [23] by solving Phonon Boltzmann Transport Equation (PBTE) [24] in single mode relaxation time approximation (SMRT) [25] and also exactly using an iterative solution [26]. Thermal conductivity(k) based on solving PBTE in SMRT approximation is given as

$$k = \frac{\hbar^2}{N\Omega k_b T^2} \sum_{\lambda} c_{a\lambda}^2 \omega_{\lambda}^2 \overline{n}_{\lambda} (\overline{n}_{\lambda} + 1) \tau_{\lambda}$$
 (1)

E-mail address: rajumenr@ou.edu (R. Muthaiah).

^{*} Corresponding author.

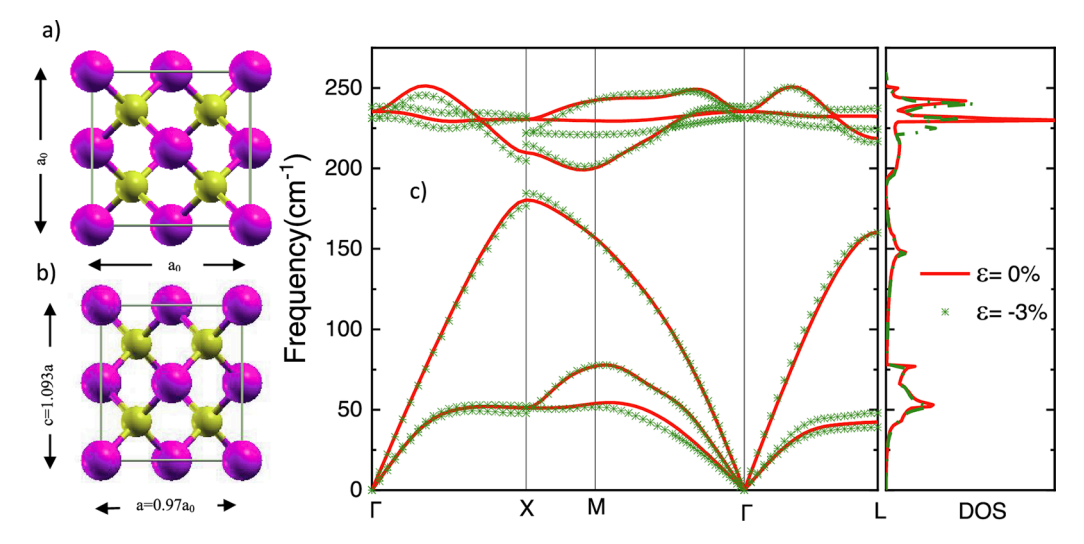


Fig. 1. Indium Arsenide with a) 0% and b) 3% strain c) Phonon dispersion and density of states for unstrained and 3% biaxially compressed InAs..

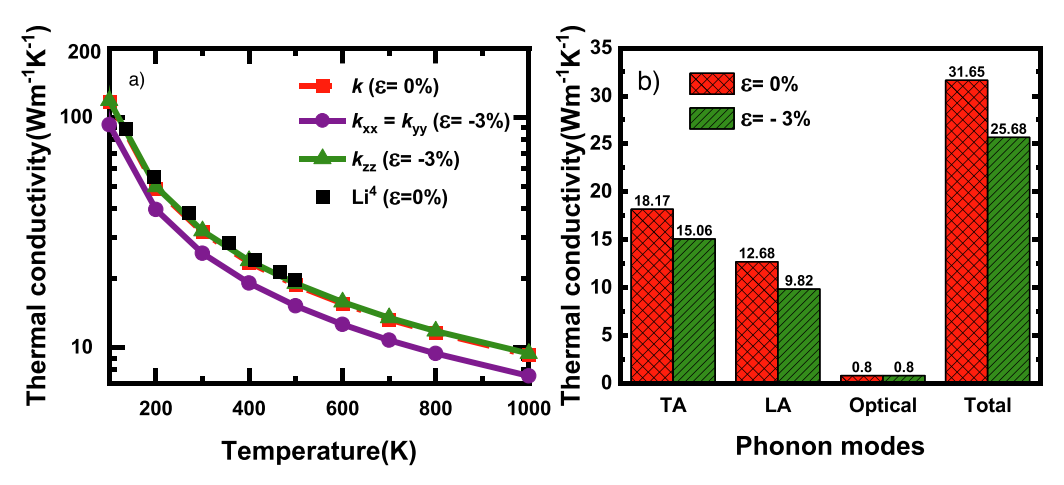


Fig. 2. a) In-plane and out-of-plane thermal conductivity of 0%, 3% biaxially compressed InAs which is in good agreement with Ref. [4] at 0% strain. b) TA, LA and optical phonon mode contribution to overall thermal conductivity.

where, \hbar ,N, Ω ,k_b,T, c, ω , \overline{n} , and τ are the are the plank constant, size of the q-point mesh, primitive unit cell volume, Boltzmann constant, absolute temperature, phonon group velocities, phonon frequencies, Bose-Einstein equilibrium populations, and the relaxation time respectively. 2nd and 3rd order force constants were derived from the density functional theory (DFT) [27] using QUANTUM ESPRESSO [28]. Normconserving pseudopotentials were used in the local density approximation (LDA) [29] and with a plane-wave cut off of 90 Rydberg. Cubic InAs was relaxed until the residual stress and forces acting on the atoms became zero. The computed equilibrium lattice constant of 5.967 Å is in good agreement with the previously reported first-principles values [30]. A Monkhorst *k*-point mesh of $12 \times 12 \times 12$ were used to describe the electronic properties during self-consistent calculations [31]. To compute the dynamical matrix and 2^{nd} order force constants $8 \times 8 \times 8$ qgrid were used. $4 \times 4 \times 4$ q-grid were used to compute the 3^{rd} order force constants using QUANTUM ESPRESSO D3Q [32,33] package. Acoustic sum rules were imposed on both 2nd and 3rd order force constants. Phonon group velocities, frequencies and Bose-Einstein populations were calculated using 2nd order force constants and phonon lifetimes were calculated using both 2nd and 3rd order interatomic force constants. $30\,\times\,30\,\times\,30$ q-mesh was used to calculate phonon linewidths and thermal conductivity and the solution of Boltzmann transport equation was found to be converged after 8 iterations.

To study the effect of strain, 3% biaxial compressive strain was

applied along x-y direction and the structure was relaxed in z-direction to eliminate residual stress. Phonon dispersions for the unstrained and 3% biaxial strained InAs are compared in Fig. 1. We can observe changes in phonon band gap between acoustic and optical phonons. Phonon band gap for the unstrained InAs is $18.65~\rm cm^{-1}$, while for 3% biaxially strained case, it was found to be reduced by 11.62% to $16.48~\rm cm^{-1}$. For ease of discussion, we have presented data for unstrained and 3% biaxial compressive strain and additional thermal transport data for 1% and 2% biaxial compressive strains are shown in supplementary information (S1). We have also reported the electronic properties such as band structure (S2), electrical conductivity (S3a) and Seebeck coefficient (S3b) in the supplementary information.

3. Results

3.1. Lattice thermal conductivity

Lattice thermal conductivity of InAs was calculated by solving Boltzmann transport equation (BTE) using both single mode relaxation approximation and exactly using iterative solution [34]. For convenience, we have shown only the exact solution in Fig. 2a. The computed values are shown in Fig. 2a and are in good agreement with the previously reported [4] first principles calculations for unstrained InAs. At 300 K, thermal conductivity(k) of unstrained InAs is 33.85 Wm⁻¹K⁻¹

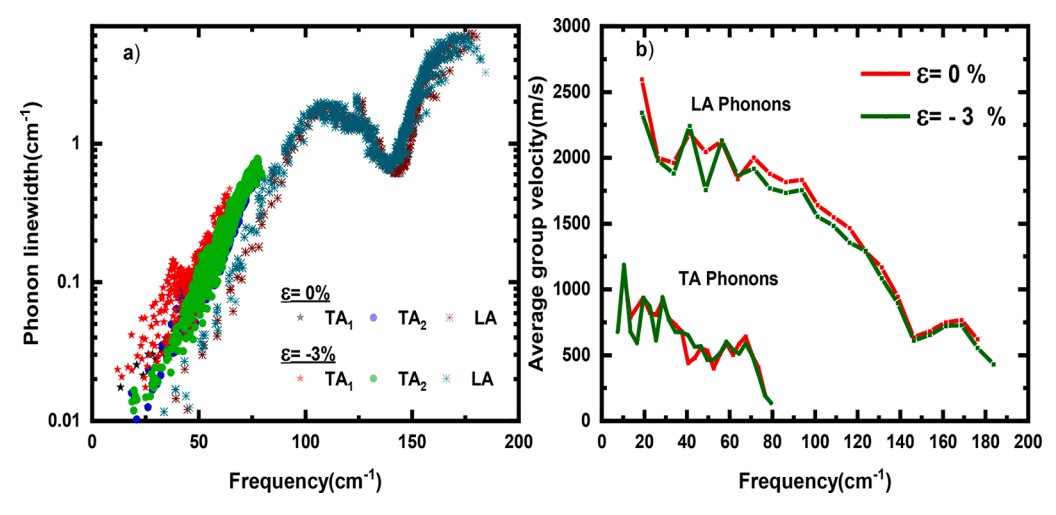


Fig. 3. a) Phonon linewidth (inverse of lifetime) and b) average phonon group velocity of InAs with 0% and 3% strain.

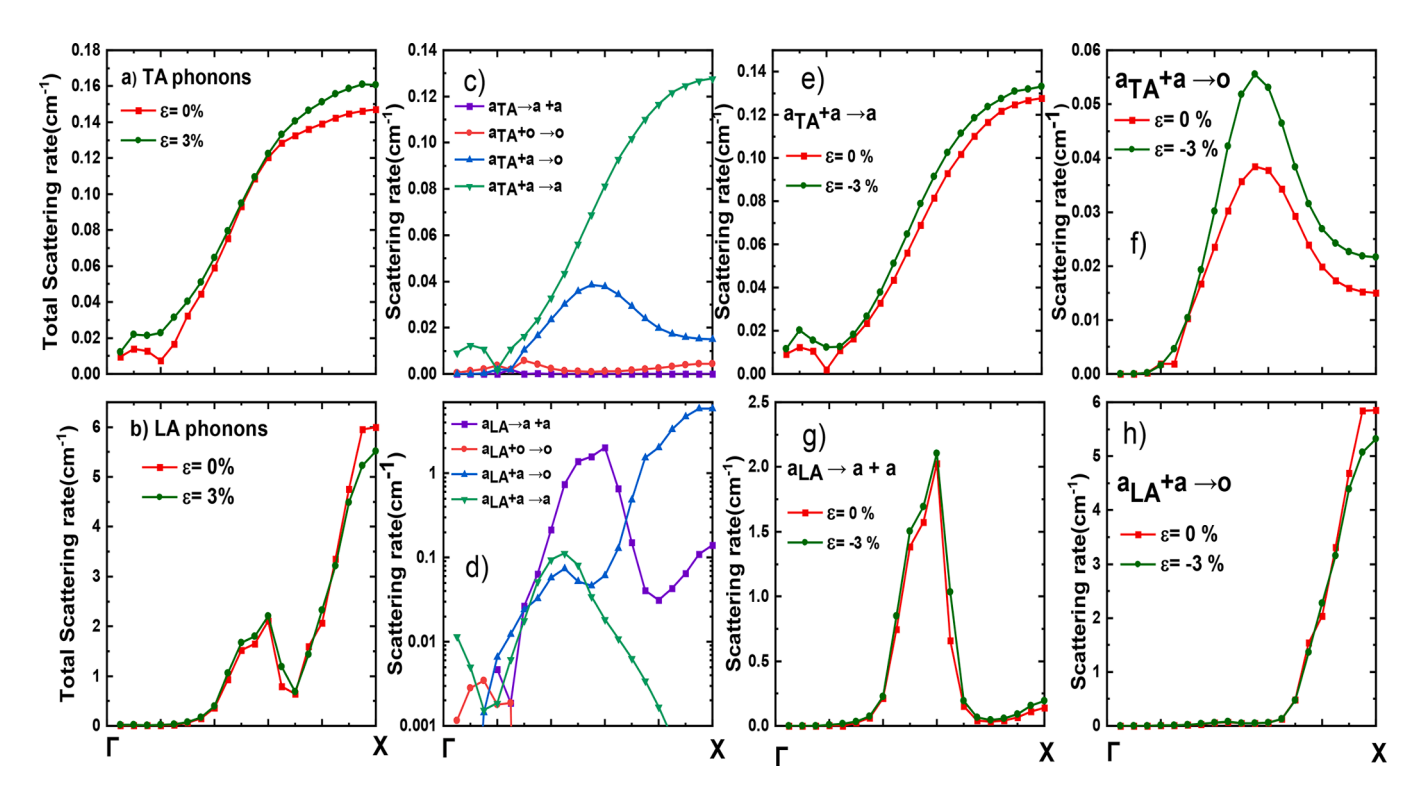


Fig. 4. a) and b) Total scattering rate of TA and LA phonon modes, respectively, c) and d) dominant scattering channels of TA and LA phonon modes, respectively, e) and f) scattering of TA phonon modes due to $a+a \rightarrow a$ and $a+a \rightarrow b$ or respectively, g) and h) scattering of LA phonons due to $a+a \rightarrow b$ and $a+a \rightarrow b$ respectively for the 0% and 3% biaxial compressive strained InAs.

which is reduced to 27 $\rm Wm^{\text{-}1} \rm K^{\text{-}1}$ along in-plane direction (a decrease of 20.23%).

Fig. 2b shows the mode contribution of TA, LA and optical phonons to overall thermal conductivity. We can observe a reduction in thermal conductivity in both TA and LA phonon modes with strain. With 3% biaxial compressive strain, thermal conductivity (k) of TA phonon mode contribution drops from 18.17 Wm⁻¹K⁻¹ to 15.06 Wm⁻¹K⁻¹ and LA phonon mode drops from 12.68 Wm⁻¹K⁻¹ to 9.82 Wm⁻¹K⁻¹. Optical phonon modes have less than ~2.5% contribution to overall thermal conductivity. To understand this reduction in thermal conductivity, we compare the phonon linewidths (inverse of phonon lifetime) and phonon group velocities of TA and LA phonon modes, as shown in Fig. 3a and b respectively. From 3a we can observe an increase in phonon scattering rates of both TA and LA phonon modes with 3%

biaxial compressive strain. In Fig. 3b, a small reduction in phonon group velocity of LA phonons is observed. Hence, *k* reduction of both TA and LA phonons are due to the combined effect of increase in phonon scattering rate and decrease in phonon group velocity.

Intrinsic three-phonon anharmonic phonon scattering can be categorized into absorption and decay processes. During the absorption process, a phonon mode $(q\omega)$ scatters by absorbing another phonon mode $(q'\omega')$ and yielding a higher energy phonon mode $(q''\omega'')$. During the decay process, a phonon mode $(q\omega)$ decays into two lower energy phonons. Both absorption and decay processes satisfy energy and momentum conservation. For example, an absorption process has to satisfy both energy $(\omega+\omega'=\omega'')$ and momentum (q+q'=q'') conservation. Similarly, decay process has to satisfy energy $(\omega=\omega'+\omega'')$ and momentum (q=q'+q'') conservation.

Fig. 4a and b represent the total scattering rate of TA and LA mode for unstrained and strained cases along Γ -X. For the 3% biaxial compressive strain, we can observe an increase in total scattering rate of TA phonons throughout Γ -X. To elucidate this increase in TA phonon modes, we have analyzed the dominant scattering channels of TA phonon modes as shown in Fig. 4c. Fig. 4c and d represent all the possible phonon scattering channels of TA and LA phonon mode for unstrained InAs such as, a) an acoustic mode decaying into two acoustic phonons (a \rightarrow a + a), b) an acoustic phonon absorbing an optical phonon to yield higher energy optical phonon (a + o \rightarrow o), c) an acoustic phonon absorbing another acoustic phonon yielding higher energy optical phonons (a + a \rightarrow o) and d) an acoustic phonon absorbing another acoustic phonons yielding a higher energy acoustic phonon (a + a \rightarrow a).

From Fig. 4c, we can observe that, the dominant phonon scattering channels of TA modes are $a + a \rightarrow a$ and $a + a \rightarrow o$. The scattering rates of both these modes increase with applied strain (shown in Fig. 4e and f). For an example, at q = 0.55 (reduced units) along Γ -X, scattering due to $a + a \rightarrow o$ mode is found to increase by 50%. Dominant scattering channels for LA phonons are $a + a \rightarrow o$ and $a \rightarrow a + a$ (Fig. 4d). The effect of strain on these channels is shown in 4 g and f. k reduction of LA phonons is due to the combined effect of reduction in phonon group velocities and increase in phonon scattering.

4. Conclusion:

In summary, using first-principles calculations and by solving Phonon Boltzmann Transport Equation iteratively, we have studied the thermal transport in biaxially strained Indium Arsenide (InAs). Thermal conductivity (k) of 3% biaxial compressively strained InAs reduced by \sim 20% along in-plane direction. Phonon group velocity and phonon scattering rate of TA and LA phonon modes upon strain were investigated and our first principles calculations reveal that reduction in k is due to a combination of increase in phonon scattering rate and decrease in phonon group velocity of both TA and LA phonons. These results provide an avenue for improving the thermoelectric performance by reducing the lattice thermal conductivity through biaxial strain.

CRediT authorship contribution statement

Rajmohan Muthaiah: Conceptualization, Methodology, Data curation, Writing - original draft. **Jivtesh Garg:** Funding acquisition, Project administration, Writing - review & editing, Supervision, Validation.

Declaration of Competing Interest

The authors declare that they have no known competing financial interests or personal relationships that could have appeared to influence the work reported in this paper.

Acknowledgements

R.M and J.G would like to acknowledge OU Supercomputing Center for Education Research (OSCER) for providing computational resources. JG acknowledges financial support from NSF CAREER grant (#1847129).

Appendix A. Supplementary data

Supplementary data to this article can be found online at https://doi.org/10.1016/j.commatsci.2021.110531.

References

[1] G. Tan, M. Ohta, M.G. Kanatzidis, Thermoelectric power generation: from new materials to devices, Philos. Trans. Roy. Soc. A: Math. Phys. Eng. Sci. 377 (2152) (2019) 20180450.

- [2] J. He, T.M. Tritt, Advances in thermoelectric materials research: Looking back and moving forward, Science 357 (6358) (2017) eaak9997.
- [3] X. Zhang, L.-D. Zhao, Thermoelectric materials: Energy conversion between heat and electricity, J. Materiomics 1 (2) (2015) 92–105.
- [4] F. Zhou, A.L. Moore, J. Bolinsson, A. Persson, L. Fröberg, M.T. Pettes, H. Kong, L. Rabenberg, P. Caroff, D.A. Stewart, N. Mingo, K.A. Dick, L. Samuelson, H. Linke, L. Shi, Thermal conductivity of indium arsenide nanowires with wurtzite and zinc blende phases, Phys. Rev. B 83 (20) (2011), 205416.
- [5] G.J. Snyder, A.H. Snyder, Figure of merit ZT of a thermoelectric device defined from materials properties, Energy Environ. Sci. 10 (11) (2017) 2280–2283.
- [6] W. Liu, X. Tan, K. Yin, H. Liu, X. Tang, J. Shi, Q. Zhang, C. Uher, Convergence of Conduction Bands as a Means of Enhancing Thermoelectric Performance of \$n \$-Type \${\mathrm{Mg}}_{2}{\mathbb{Q}}{\mathbb{q}}_{1}ensuremath{-}x}{\mathbb{S}}_{x}\$ Solid Solutions, Phys. Rev. Lett. 108 (16) (2012), 166601.
- [7] Y. Pei, X. Shi, A. LaLonde, H. Wang, L. Chen, G.J. Snyder, Convergence of electronic bands for high performance bulk thermoelectrics, Nature 473 (7345) (2011) 66–69.
- [8] K. Biswas, J. He, Q. Zhang, G. Wang, C. Uher, V.P. Dravid, M.G. Kanatzidis, Strained endotaxial nanostructures with high thermoelectric figure of merit, Nat. Chem. 3 (2) (2011) 160–166.
- [9] B. Poudel, Q. Hao, Y. Ma, Y. Lan, A. Minnich, B. Yu, X. Yan, D. Wang, A. Muto, D. Vashaee, X. Chen, J. Liu, M.S. Dresselhaus, G. Chen, Z. Ren, High-thermoelectric performance of nanostructured bismuth antimony telluride bulk alloys, Science 320 (5876) (2008) 634–638.
- [10] X. Hu, P. Jood, M. Ohta, M. Kunii, K. Nagase, H. Nishiate, M.G. Kanatzidis, A. Yamamoto, Power generation from nanostructured PbTe-based thermoelectrics: comprehensive development from materials to modules, Energy Environ. Sci. 9 (2) (2016) 517–529.
- [11] L.-D. Zhao, G. Tan, S. Hao, J. He, Y. Pei, H. Chi, H. Wang, S. Gong, H. Xu, V. P. Dravid, C. Uher, G.J. Snyder, C. Wolverton, M.G. Kanatzidis, Ultrahigh power factor and thermoelectric performance in hole-doped single-crystal SnSe, Science 351 (6269) (2016) 141–144.
- [12] L. Yang, Z.-G. Chen, M. Hong, G. Han, J. Zou, Enhanced thermoelectric performance of nanostructured Bi2Te3 through significant phonon scattering, ACS Appl. Mater. Interfaces 7 (42) (2015) 23694–23699.
- [13] S. Bathula, M. Jayasimhadri, N. Singh, A.K. Srivastava, J. Pulikkotil, A. Dhar, R. C. Budhani, Enhanced thermoelectric figure-of-merit in spark plasma sintered nanostructured n-type SiGe alloys, Appl. Phys. Lett. 101 (21) (2012), 213902.
- [14] Y. Xiao, L.-D. Zhao, Charge and phonon transport in PbTe-based thermoelectric materials, npj Quantum Mater. 3 (1) (2018) 55.
- [15] B. Jiang, X. Liu, Q. Wang, J. Cui, B. Jia, Y. Zhu, J. Feng, Y. Qiu, M. Gu, Z. Ge, J. He, Realizing high-efficiency power generation in low-cost PbS-based thermoelectric materials, Energy Environ. Sci. 13 (2) (2020) 579–591.
- [16] R. Muthaiah, J. Garg, Strain tuned high thermal conductivity in boron phosphide at nanometer length scales a first-principles study, PCCP (2020).
 [17] D.-S. Tang, G.-Z. Qin, M. Hu, B.-Y. Cao, Thermal transport properties of GaN with
- [17] D.-S. Tang, G.-Z. Qin, M. Hu, B.-Y. Cao, Thermal transport properties of GaN with biaxial strain and electron-phonon coupling, J. Appl. Phys. 127 (3) (2020), 035102.
- [18] I.R. Grant, III–V Compound Semiconductors: Growth, in: K.H.J. Buschow, R. W. Cahn, M.C. Flemings, B. Ilschner, E.J. Kramer, S. Mahajan, P. Veyssière (Eds.), Encyclopedia of Materials: Science and Technology, Elsevier, Oxford, 2001, pp. 1441–1452.
- [19] A.G. Milnes, A.Y. Polyakov, Indium arsenide: a semiconductor for high speed and electro-optical devices, Mater. Sci. Eng., B 18 (3) (1993) 237–259.
- [20] N. Kaiwa, J. Yamazaki, T. Matsumoto, M. Saito, S. Yamaguchi, A. Yamamoto, Thermoelectric properties and a device based on n-InSb and p-InAs, Appl. Phys. Lett. 90 (5) (2007), 052107.
- [21] R. Bowers Jr., R. W. U., Bauerle, J. E., Cornish, A. J., InAs and InSb as Thermoelectric Materials, J. Appl. Phys. 30 (6) (1959) 930–934.
- [22] P.M. Wu, J. Gooth, X. Zianni, S.F. Svensson, J.G. Gluschke, K.A. Dick, C. Thelander, K. Nielsch, H. Linke, Large thermoelectric power factor enhancement observed in InAs nanowires, Nano Lett. 13 (9) (2013) 4080–4086.
- [23] J. Garg, N. Bonini, N. Marzari, First-principles determination of phonon lifetimes, mean free paths, and thermal conductivities in crystalline materials: pure silicon and germanium, in: S.L. Shindé, G.P. Srivastava (Eds.), Length-Scale Dependent Phonon Interactions, Springer, New York: New York, NY, 2014, pp. 115–136.
- [24] J. Garg, N. Bonini, B. Kozinsky, N. Marzari, Role of disorder and anharmonicity in the thermal conductivity of silicon-germanium alloys: a first-principles study, Phys. Rev. Lett. 106 (4) (2011), 045901.
- [25] A.J.H. McGaughey, M. Kaviany, Quantitative validation of the Boltzmann transport equation phonon thermal conductivity model under the single-mode relaxation time approximation, Phys. Rev. B 69 (9) (2004), 094303.
- [26] A.C. Sparavigna, The variational principle and the phonon Boltzmann equation, Mech. Mater. Sci. Eng. 8 (2017).
- [27] A. Debernardi, S. Baroni, E. Molinari, Anharmonic phonon lifetimes in semiconductors from density-functional perturbation theory, Phys. Rev. Lett. 75 (9) (1995) 1819–1822.
- [28] P. Giannozzi, S. Baroni, N. Bonini, M. Calandra, R. Car, C. Cavazzoni, D. Ceresoli, G.L. Chiarotti, M. Cococcioni, I. Dabo, A. Dal Corso, S. de Gironcoli, S. Fabris, G. Fratesi, R. Gebauer, U. Gerstmann, C. Gougoussis, A. Kokalj, M. Lazzeri, L. Martin-Samos, N. Marzari, F. Mauri, R. Mazzarello, S. Paolini, A. Pasquarello, L. Paulatto, C. Sbraccia, S. Scandolo, G. Sclauzero, A.P. Seitsonen, A. Smogunov, P. Umari, R.M. Wentzcovitch, QUANTUM ESPRESSO: a modular and open-source software project for quantum simulations of materials, J. Phys.: Condens. Matter 21 (39) (2009), 395502.

- [29] J.-L. Calais, Density-functional theory of atoms and molecules. R.G. Parr and W. Yang, Oxford University Press, New York, Oxford, 1989. IX + 333 pp. Price £45.00. Int. J. Quantum Chem. 1993, 47 (1), 101-101.
- [30] J. Garg, I.R. Sellers, Phonon linewidths in InAs/AlSb superlattices derived from first-principles—application towards quantum well hot carrier solar cells, Semicond. Sci. Technol. 35 (4) (2020), 044001.
- [31] H.J. Monkhorst, J.D. Pack, Special points for Brillouin-zone integrations, Phys. Rev. B 13 (12) (1976) 5188–5192.
- [32] L. Paulatto, I. Errea, M. Calandra, F. Mauri, First-principles calculations of phonon frequencies, lifetimes, and spectral functions from weak to strong anharmonicity: The example of palladium hydrides, Phys. Rev. B 91 (5) (2015), 054304.
- [33] L. Paulatto, F. Mauri, M. Lazzeri, Anharmonic properties from a generalized thirdorder ab initio approach: Theory and applications to graphite and graphene, Phys. Rev. B 87 (21) (2013), 214303.
- [34] M. Omini, A. Sparavigna, Beyond the isotropic-model approximation in the theory of thermal conductivity, Phys. Rev. B 53 (14) (1996) 9064–9073.
- [35] G.K.H. Madsen, D.J. Singh, BoltzTraP, A code for calculating band-structure dependent quantities, Comput. Phys. Commun. 175 (1) (2006) 67–71.